HHS Public Access

Author manuscript

EuPA Open Proteom. Author manuscript; available in PMC 2016 September 01.

Published in final edited form as:

EuPA Open Proteom. 2015 September ; 8: 40–47. doi:10.1016/j.euprot.2015.05.005.

Reducing protein oxidation in low-flow electrospray enables deeper investigation of proteoforms by top down proteomics

Kyunggon Kim[a], **Philip D. Compton**[a], **Timothy K. Toby**[a], **Paul M. Thomas**[a], **John T. Wilkins**[b,c], **R. Kannan Mutharasan**[c], and **Neil L. Kelleher**[a,*]

[a]Departments of Chemistry, Molecular Biosciences and the Proteomics Center of Excellence, Northwestern University, 2145 N. Sheridan Road, Evanston, IL 60208, United States

[b]Department of Preventive Medicine, Northwestern University Feinberg School of Medicine, 680 N. Lake Shore Drive., Chicago, IL 60611, United States

[c]Department of Medicine, Division of Cardiology, Northwestern University Feinberg School of Medicine, 676 N. Saint Clair Street, Chicago, IL 60611, United States

Abstract

Enabling the implementation of top down proteomic techniques within clinical workflows requires a dramatic increase in sensitivity. It has been previously demonstrated that electrospray ionization (ESI) becomes more efficient with decreasing volumetric flow rates at the emitter. Therefore, narrow inner diameter (I.D.) columns used in front-end chromatographic separations yield increased sensitivity. However, the smaller cross-sectional area of a narrow I.D. column places a larger fraction of the eluent in fluid communication with the electrode within the high voltage union that facilitates electrospray ionization (ESI), leading to increased oxidation of solution-phase proteins. Oxidation of proteins alters their chemical state of the protein, complicates data analysis, and reduces the depth of proteome coverage attained in a typical top-down proteomics experiment. Excessive protein oxidation results in poor deconvolution and exact mass calculations from MS1 spectra, interferes with peak isolation for MS/MS fragmentation, and effectively reduces sensitivity by splitting ion current. All of these factors deteriorate top down mass spectral data quality, an effect that becomes more pronounced as column diameter decreases. Artificial protein oxidation can also mislead investigations of *in vivo* protein oxidation. All of these effects are accentuated in comparison to bottom up proteomics due to the increased probability of having oxidizable residues within a particular species with increasing mass. Herein, we describe a configuration (which we term “Low Protein Oxidation (LPOx)”) for proteomics experiments created by re-arranging liquid chromatography (LC) plumbing and present its application to artificial protein oxidation and show a marked improvement in detection sensitivity. Using a

*Corresponding author. Tel.: +1 847 467 4362; fax: +1 847 467 3276. n-kelleher@northwestern.edu (N.L. Kelleher).

Author contributions

KK, PDC, PMT, TKT and NLK wrote the manuscript, KK, JTW and RKM performed experiments and data analysis. PDC suggested the concept for the experiment. All authors have given approval to the final version of the manuscript.

Notes

The authors declare competing financial interests. Qualitative protein analyses were performed in ProSightPC, a product commercialized by the Kelleher Research Group.

standard mixture of five intact proteins, we demonstrate that the LPOx configuration reduces protein oxidation up to 90% using 50 μm I.D. columns when compared to a conventional LC plumbing configuration with 50 μm I.D. column. As a proof-of-concept study, at least 11 distinct proteoforms of serum Apolipoprotein A1 were detected with the LPOx configuration. This innovative LC configuration can be applied to the top down identification and characterization of proteoforms obscured by abundant artificial protein oxidation at low flowrates, all while using reduced amounts of valuable protein samples.

Keywords

Top down; Protein oxidation; Proteoforms; Electrospray ionization

1. Introduction

The analysis of intact proteins with high-resolution mass spectrometry combined with post-data analysis has provided qualitative and more recently, quantitative information on the proteomes of various organisms [1–5]. Thorough amino acid sequence coverage and post-translational modification (PTM) identity and location can be obtained from the combination of highly accurate intact masses yielded by MS1 spectra and MS/MS fragment ion masses generated by fragmentation, facilitating the discovery of proteoforms unique to specific biologic conditions [6]. As the capabilities of top down proteomics have expanded, the approach is now beginning to realize its potential as a disruptive clinical methodology. One of the most important, emerging roles for top down proteomics in this capacity has been the discovery of disease-related, proteoform-resolved biomarkers, which may serve as diagnostic or prognostic indicators, targets for therapy, and markers of therapeutic efficacy [7].

Even after a series of major advancements in mass spectrometry instrumentation, including the development of high-resolution mass spectrometers and nano-flow liquid chromatography (nLC), the limited amount of protein sample that can be obtained from patients (biopsied tissue, sorted cells from blood, banked serum from large scale epidemiologic studies, etc.) has remained a barrier for intensive, large-scale biomarker research by top down proteomics. Over the past several decades, the development and application of narrow inner diameter columns to front-end LC separations has presented an effective option to improve sensitivity in sample limited situations [8–9]. In the past, Ye, et al. showed that a 2.1 mm I.D. column yields up to a seven-fold increase in sensitivity compared to a 4.6 mm I.D. column for α-, β-, γ-, and δ-tocopherol analysis using micro flow [10]. Emmett reported that micro-ESI needles of 25–50 μm inner diameter coupled with FT-ICR system produced mass spectra from a mixture of three neuroactive peptides at a concentration of 500 amol/μL in biological salts with baseline separation, signal-to-noise ratio of >10:1 and mass resolving power >5000 [11]. Further, Luo et al. reported that reducing the inner diameter to 10 μm monolithic columns increased the sensitivity of peptide detection by 10-fold using flow rates as low as 10 nL/min [12]. In Luo's result, it was shown that narrow I.D. analytical columns better concentrate low sample volumes for optimal detection by LC–MS, and, when combined with nano-flow rates that enhance ionization

efficiency, result in >5000 different peptides identification from 100 ng of a *Shewanella oneidensis* tryptic digest.

Typical top down proteomics experiments employ 100 μm or 75 μm I.D. columns connected via a vented tee configuration to bind, wash, and separate proteins for analysis (Fig. 1A) [13]. However, when narrower 50 μm I.D. columns are applied to this configuration to take advantage of the known increase in sensitivity for limited sample amounts, the unwelcome phenomenon of protein oxidation occurs more readily than in 75 μm I.D. columns. The 2.2-fold reduction in cross-sectional area results in a higher proportion of the mobile phase interacting with the ESI electrode. As the eluting proteins pass through this junction, the redox processes occurring at the electrode can lead to oxidation. Oxidation of peptides and proteins during electrospray ionization has been known for over 20 years [14]. Oxidation typically manifests itself as a series of 15.995 Da mass increases from the original unmodified mass spectral peak of the proteoforms of interest.

Protein oxidation is not only a chemical artifact of LC–MS but also an important potential *in vivo* modification [15,16]. Oxidative stress associated with aging and certain disease conditions can oxidize proteins and thereby modulate their functions to a physiologically significant degree, either by inhibiting enzymatic and binding activities, increasing susceptibility to aggregation and proteolysis, changing uptake rates by cells, or altering immunogenicity [17]. For example, Wright et al. demonstrated that long-lived Tyr-derived peroxides are formed on proteins exposed to $^1O_2$, and that these modified proteoforms may promote damage to other targets via further radical generation [18,19]. Also, Yeong-Renn et al. showed that protein oxidation of cytochrome c by reactive halogen species enhances its peroxidase activity [20]. While the natural, *in vivo* oxidation of proteins is clearly an important PTM that may inform the study of various human diseases, it is impossible to distinguish *in vivo* oxidation from the *in situ* protein oxidation that occurs artificially at the high voltage union in LC–ESI–MS. Therefore, it is important to minimize or eliminate instrument-related protein oxidation in order to study *in vivo* protein oxidation with top down LC–MS.

Apolipoprotein A1, as a major component of high-density lipoproteins (HDL), is reported to protect against atherosclerosis via several mechanisms, including its ability to mediate the first step in reverse cholesterol transport, the efflux of cholesterol from lipid-laden macrophages [21]. Additionally, an inverse relationship between Apolipoprotein A1 serum levels and coronary heart disease has been observed [22,23]. Oxidation of Apolipoprotein A1 has been demonstrated both *in vitro* [24] and *in vivo* [25], and has been shown to be functionally significant, decreasing cholesterol efflux in *ex vivo* assays of reverse cholesterol transport [23,25,26]. Mateos-Caceres et al. have reported on the five isoforms of plasma apolipoprotein A1 in patients suffering from acute coronary syndrome using 2-dimensional electrophoresis (2-DE), but the method could not elucidate important information regarding the PTMs present on these isoforms [27]. It is known that apolipoprotein A1 is processed to three different lengths, including a pro-form (amino acids 19-276), a mature form (25-267), and a truncated form (25-266), and can be modified by *in vivo* oxidation at multiple methionine, tyrosine and tryptophan residues within the protein as well as by N-linked glycosylation at Lys-263 [24,28,29]. There are 26 reported natural apolipoprotein A1 forms

which vary at 24 different amino acid positions, making the complete top down analysis of apolipoprotein A1 in individual patients quite a challenge [30–33]. The development of highly sensitive methods to prevent *in situ* instrumental oxidation and then detect and characterize oxidative proteoforms of apolipoprotein A1, not to mention the myriad other proteins oxidized by biological processes *in vivo*, remains an unmet need.

In this study, an LC configuration using 50 μm I.D. columns was utilized to reduce artificial protein oxidation levels and increase sensitivity for top down proteomic analysis. MS data for a standard five protein mixture were obtained with the LPOx configuration using 50 μm I.D. analytical columns and compared to the conventional setting using both 75 μm and 50 μm I.D. columns. As a proof-of-concept, human serum apolipoprotein A1 was analyzed using the novel LPOx configuration to determine its performance and applicability to valuable clinical sample sets.

2. Materials and methods

2.1. Standard protein mixture

A “Top Down Standard” mixture containing 0.1 pmol ubiquitin, 0.5 pmol trypsinogen, 1 pmol myoglobin, and 0.5 pmol carbonic anhydrase (all Sigma–Aldrich, St. Louis, MO) was freshly prepared in LC–MS Buffer A (95% water, 5% acetonitrile, and 0.2% formic acid). Superoxide dismutase (SOD) occurs as a contaminant from the purchased preparation of carbonic anhydrase.

2.2. Apolipoprotein enrichment using PHM-L Liposorb absorbent

Two young male healthy donors provided serum for analysis in a protocol approved by the Institutional Review Board at Northwestern University (IRB No. STU00097261). Blood was obtained by venipuncture into BD Serum Separator tubes (Becton Dickinson, East Rutherford, NJ), gently inverted five times, allowed to stand at room temperature for 30 min, then centrifuged at 1100 × *g* for 10 min to separate the serum fraction. Serum was then stored at −80°C. Serum (20 μL) and 4 mg of PHM-L LIPOSORB^{TM} absorbent (Millipore; Billerica, MA) were combined in 1 mL of 100 mM ammonium bicarbonate (Sigma–Aldrich) and mixed in a shaking incubator for 30 min at room temperature. After the absorbent was washed 3 times with 100 mM ammonium bicarbonate, bound apolipoproteins were eluted with 100 μL 5% sodium dodecyl sulfate (SDS) solution. SDS in the sample was then removed by protein precipitation in methanol, chloroform, and water as previously described [13]. The resultant dried protein pellet was reconstituted in 50 μL of Buffer A (5% acetonitrile in water +0.2% formic acid) before MS analysis.

2.3. Capillary plumbing

Flexible fused silica capillary tubing for trap columns (O.D.: 360 μm, I.D.: 150 μm) and analytical columns (O.D.: 360 μm, I.D.: 50 μm and 75 μm) were purchased from Polymicro Technologies (Phoenix, AZ). Polymeric reverse-phase (PLRP-S, d_P = 5 μm, pore size = 1000 Å, Agilent Technologies; Santa Clara, CA) [34] was packed in fritted capillary tubing to make trap columns (packing length: 2 cm) and analytical columns (packing length: 15 cm) using a home-made pressure cell. Spray emitters (360 μm O.D., 50 μm I. D., 8 μm tip,

Cat. No: FS360-50-8-N-20) were purchased from New Objective (Woburn, MA) and micro tee assemblies (Cat. No: P-888) for vented tees were purchased from Upchurch Scientific (Oak Harbor, WA). Conventional LC plumbing was installed as shown in Fig.1A. Briefly, the trap column, vented tee, analytical column, high voltage tee and spray emitter were assembled in order from the switching valve. The novel LPOx plumbing was assembled as shown in Fig. 1B. The stator for the 10-port switching valve (SV2) (Cat. No: 6041.0012) was purchased from Dionex (Sunnyvale, CA). The dimensions of all capillaries which have not been mentioned are: O.D. 360 μm and I.D 30 μm. Valve switching of SV1 and SV2 were programmed into the LC method using the Chromeleon chromatography data system (Dionex, version 6.8)

2.4. Mass spectrometry analysis

Resuspended protein fractions (5 μL) were injected onto a trap column using an autosampler (Dionex). A nanobore analytical column (75 μm or 50 μm I.D.) was coupled to the trap in a vented tee setup. For the conventional capillary setting, a Dionex Ultimate 3000 RSLCnano system was operated at a flow rate of 2.5 μL/min for loading sample onto the trap. Proteins were separated on the analytical column and eluted into the mass spectrometer using a flow rate of 300 nL/min for 75 μm I.D. column and 100 nL/min for 50 μm I.D. column using the following gradient: 5% B at 0 min; 15% B at 5 min; 55% B at 55 min; 95% B from 58 to 61 min; 5% B from 64 to 80 min (Solvent B: 5% water, 95% acetonitrile, 0.2% formic acid). For the 50 μm I.D. LPOx configuration, all LC parameters were identical to the conventional setting except the flow rate (700 nL/min) and the use of a flow restrictor (O.D.: 360 μm, I.D: 10 μm, length: 10 cm). Measured flow rate at the end of the emitter was ~ 100 nL/min.

Mass spectrometry data were obtained on an Orbitrap Elite mass spectrometer fitted with a custom nanospray ionization source. For the MS method, the FTMS data were collected (4 microscans, *m*/*z* 500–2000, resolution 120,000). For data-dependent MS/MS, the top 2 peaks in the full-scan FT spectrum were fragmented using higher-energy collisional dissociation (HCD) with normalized collision energy of 25, isolation width of 50 *m*/*z*, 4 microscans and a resolving power of 60,000. Dynamic exclusion was performed with a repeat count of 2, a repeat duration of 120 s and an exclusion duration of 5000 s. Automatic gain control (AGC) was set to 1E6 ions and the maximum injection time was set to 1 s for both MS and MS/MS. A 15 V offset in the source was used throughout the entire experiment. The capillary temperature was 320 °C and the spray voltage was set to 2.0 kV.

2.5. Data processing

Data from the mass spectrometer were submitted to a distributed version of ProSightPC 3.0 (Thermo Fisher Scientific; Waltham, MA) using a custom database built from the five protein sequences. Mass tolerances for both precursor ions and fragment ions were set to 10 ppm [3]. E-values and the number of fragment ions (*b* and *y* ions only) reported in the ProSightPC 3.0 results were used to benchmark confident proteoform identifications.

3. Results and discussion

3.1. High voltage tee arrangement and LC flow splitting in the LPOx configuration

For the conventional capillary setting shown in Fig. 1A, only a single switching valve (SV1) was used. During the LC loading step, a 2.5 μL/min flow brings sample into the trap column where proteins are bound and washed. The resulting solvent waste goes through the vented tee without any applied ESI voltage. During the gradient, an SV1 valve switch blocks the vented tee and proteins in the trap column are eluted onto the analytical column and separated at 300 nL/min for 75 μm I.D. column and 100 nL/min flow for 50 μm I.D. column, respectively.

In the LPOx configuration, a high voltage tee is located prior to a preliminary vented tee (VT1) connected to the trap column in a branched configuration (Figs.1 B, 2 A and B). During the LC loading phase, a 2.5 μL/min flow from SV1 (4 → 3) containing sample proteins can pass through VT1 (a → c), the trap column, and another vented tee (VT2; a → b), and the waste is directed through a second switching valve (SV2; 2 → 1) in the absence of high voltage. During the gradient, SV1 changes position (2 → 3) and initiates nano-flow (700 nL/min). LC flow is now divided into two streams at VT1. First, the flow stream from VT1 (a → b) to the high voltage tee (a → c) can be controlled by the backpressure of an installed restrictor. Second, the other LC flow stream from VT1 (a → c) through VT2 (a → c) can elute proteins from the trap column and separate them on the reverse-phase analytical column without any direct contact with the high voltage electrode. A 10 μm I.D. fused silica capillary with a length of 10 cm was chosen as a restrictor to modulate the flow rate of VT1 (a → c) to ~100 nL/min. A non-conductive stator for SV2 resolves an electrical grounding issue when high voltage is applied to the system.

3.2. The novel LPOx configuration with a 50 μm I.D. column yielded less oxidation of an intact protein mixture

The artificial oxidation of five proteins was investigated by analysis of their MS1 spectra after LC separation through two different analytical column diameters in the conventional and LPOx configurations with triplicate in each case. As shown in Fig. 3A, minor but distinct oxidation of ubiquitin, trypsinogen, and carbonic anhydrase was detected after their separation on a 75 μm I.D. analytical column in the conventional capillary setting. The observed 9+ ubiquitin charge state at 954.41 *m/z* is an oxidized form of the 9+ peak at 952.63 *m/z*. An extended series of oxidative peaks appear at higher *m/z* from the unmodified peaks for SOD and myoglobin. When separations were performed with the 50 μm I.D. column in the conventional capillary setting (Fig. 3B), these oxidative peaks significantly increased for all five proteins. The oxidation level of trypsinogen and carbonic anhydrase increased more than those detected with the 75 μm I.D. columns. This vast increase in protein oxidation can be explained by the difference in column cross-sectional area. As previously stated, the 2.2-times smaller cross-sectional area and lower flow rates result in higher oxidation of liquid-phase proteins. As depicted in Fig. 3C, the LPOx configuration yielded minor or no oxidation for all five proteins. In the LPOx configuration, proteins do not make direct contact with the high voltage electrode because it is located in a branched configuration upstream of the trap column, and the high voltage is transmitted by the stream

of liquid between the high voltage source and VT1. The analysis was performed using MS1 (intact protein mass spectra) as the primary readout of overall protein oxidation levels. MS2 data were collected to show the increase in confidence for protein identification of the unoxidized proteoform (*vide infra*). Percentage of oxidation for each protein was shown in Table 1. For ubiquitin, the percentage of oxidation in 75 μm I.D. and 50 μm I.D. conventional configurations were 12% and 73%, respectively, and was decreased to 3% in LPOx configuration with a 50 μm I.D. column. More significant reduction of oxidation was observed in superoxide dismutase and trypsinogen. In trypsinogen, 93% oxidation was observed using a 50 μm I.D column with conventional configuration; this declined 2% in the 50 μm I.D. column with LPOx configuration.

Database search results and MS parameters from the LPOx configuration and conventional setting using the 50 μm I.D column for ubiquitin and myoglobin were compared and are shown in Fig. 4. In LPOx configuration, an increase of unoxidized fragment ions for each protein could be observed. For ubiquitin, the number of observed fragment ions was 49.0 ± . 9 and the FT injection time was 0.30 ± 0.02 msec in LPOx configuration and in the conventional setting, the number of observed fragment ions was 41.7 ± 2.2 and FT injection time was 1.70 ± 0.23 msec. These results were consistent for myoglobin (number of fragment ions: 16.0 ± 4.68 for the conventional setting and 34.3 ± 3.2 for the LPOx configuration, FT injection time: 0.40 ± 0.06 for conventional setting and 0.30 ± 0.09 for LPOx configuration). These results can be inferred from the different peak shapes between the two results. Peaks with high intensities and narrow widths demonstrate that the mass spectrometer with AGC receives a higher ion flux and can trap ions in a shorter injection time; this facilitates the accurate isolation of proteoform ions during MS/MS to produce many fragment ions for characterization. All of these results indicate that reduced artificial protein oxidation in the LPOx configuration can improve qualitative data analysis in top down proteomics, and can be helpful for characterizing PTMs on intact proteins.

3.3. Comparison of the LPOx configuration with a 50 μm I.D. analytical column and conventional LC plumbing with a 75 μm I.D. column showed improvement in sensitivity

When artificial protein oxidation occurs, the unmodified peak intensities decrease as the original species are distributed into oxidative ion species. From this concept, it is reasonable to conjecture that peak intensities in a conventional LC set-up are lower than in the LPOx configuration. In the conventional setting, lower oxidation levels were observed on a 75 μm I.D. column than on a 50 μm I.D. column, and trypsinogen and carbonic anhydrase were less oxidized overall. Still, a comparison of the LPOx configuration with a 50 μm I.D. column to the conventional setting with the high-performing 75 μm I.D. column reveals a marked sensitivity improvement with LPOx. As shown in Fig. 5, peak intensities of myoglobin at the two different settings indicate that the 50 μm I.D. LPOx configuration yields increased sensitivity 7-fold over the 75 μm I.D. conventional setting at identical sample amounts.

3.4. Proof-of-concept: the LPOx configuration reveals hidden serum apolipoprotein A1 proteoforms

As a proof-of-concept for the LPOx configuration performance and application to clinical samples, apolipoprotein A1 was purified from human serum and analyzed by top down FT–

MS online with HPLC configured in the LPOx configuration with a 50 μm I.D. analytical column. As a point of comparison, the same experiment was performed using the conventional LC setting with a 75 μm I.D. column. Fig. 6 depicts the five minute-averaged spectra obtained from the 75 μm I.D. column/conventional capillary setting and the 50 μm I.D. column/LPOx configuration. As seen in the conventional setting experiment, several abundant oxidative peaks obscure the original proteoform peaks in the 31+ charge state (Fig. 6A). It is exceedingly difficult to distinguish the true biological proteoforms (especially those from *in vivo* oxidation experiments) from the artificial oxidation forms, and the isolation of a single peak from the spectrum for MS/MS fragmentation is technically impossible.

In the LPOx configuration experiment with the 50 μm I.D. column, the reduction of artificial protein oxidation exposed several distinct peaks representing hidden apolipoprotein A1 proteoforms (Fig. 6B). In just one charge state, at least 11 distinct peaks representing different proteoforms of serum apolipoprotein A1 were distinguishable in this spectrum. This number of proteoform candidates exceeds that reported in any previous studies [4,27]. If a very narrow isolation window is applied to yield MS/MS data, it may be possible to derive PTM information and thus fully characterize each proteoform from its resultant fragmentation data. This work to further investigate the nature of the unique apolipoprotein A1 proteoforms revealed by LPOx–LC–MS and their role in cardiovascular disease is currently in progress.

4. Conclusion

Narrow I.D. columns can accommodate low amounts of valuable clinical samples and achieve higher sensitivity for top down analysis, but issues involving increased levels of protein oxidation have hindered their widespread application. The rampant protein oxidation occurring in narrow I.D columns during ESI not only impedes the investigation of *in vivo* protein oxidation but also greatly reduces top down data quality. Overlapped oxidative peaks result in poor mass deconvolution and also complicate ion isolation in MS/MS fragmentation. The innovative LPOx configuration equipped with a narrow 50 μm I.D. column can vastly reduce protein oxidation compared to conventional LC capillary settings with 75 μm and 50 μm I.D. analytical columns. The 50 μm I.D. column LPOx configuration even showed higher peak intensities and improved sensitivity in intact protein detection over the 75 μm I.D. columns employed in the current conventional configuration in top down nLC–MS. Clearly, the LPOx configuration coupled with 50 μm I.D. columns can reduce protein sample loading amounts while maintaining high detection sensitivity, making the configuration applicable to clinical sample analysis by top down proteomics.

As a proof-of-concept for improved clinical top down proteomics employing the LPOx LC configuration, we detected serum apolipoprotein A1 proteoforms including natural oxidation forms that can compose important clinical signatures for atherosclerosis and cardiovascular disease using top down proteomics coupled with the LPOx LC setting and a 50 μm I.D. analytical column. The results of this analysis suggested that there are more than 11 detectable peaks that correspond to proteoforms of serum apolipoprotein A1 that may be physiologically relevant. In this study, we demonstrated that the novel LPOx configuration

effectively reduces artificial protein oxidation and not only facilitates the investigation of biologically oxidized proteoforms, but also the discovery of proteoforms in limited amounts of clinical sample by top down proteomics.

Acknowledgments

Funding sources

The project described was supported by Award No. P30DA018310 from the National Institute on Drug Abuse and Award No. R01GM067193 from the National Institute of General Medical Sciences.

Abbreviations

LPOx	low protein oxidation
ID	inner diameter
OD	outer diameter
VT	vented tee
HVT	high voltage tee
SV	switching valve
FT–MS	Fourier transform mass spectrometer
AGC	automatic gain control
HCD	higher energy collisional dissociation
MS	mass spectrometry
MS1	intact/precursor scan
MS2	(or MS/MS)
nLC	nano liquid chromatography
SDS	sodium dodecyl sulfate
ESI	electrospray ionization
PTM	post-translational modification
HDL	high density lipoprotein
UV–LC	liquid chromatography with ultra violet detector
NMR	nuclear magnetic resonance
2-DE	2-dimensional electrophoresis
SOD	Superoxide dismutase
PHM-L	Polyhydroxymethylene substituted by fat oxethylized alcohol
RT	room temperature

References

1. Kelleher NL. Top-down proteomics. Anal Chem. 2004; 76(11):197A–203A. [PubMed: 14697051]
2. Yates JR 3rd, Kelleher NL. Top down proteomics. Anal Chem. 2013; 85(13):6151. [PubMed: 23705843]
3. Tran JC, Zamdborg L, Ahlf DR, Lee JE, Catherman AD, Durbin KR, Tipton JD, Vellaichamy A, Kellie JF, Li M, Wu C, Sweet SM, Early BP, Siuti N, LeDuc RD, Compton PD, Thomas PM, Kelleher NL. Mapping intact protein isoforms in discovery mode using top-down proteomics. Nature. 2011; 480(7376):254–258. [PubMed: 22037311]
4. LeDuc RD, Fellers RT, Early BP, Greer JB, Thomas PM, Kelleher NL. The c-score: a bayesian framework to sharply improve proteoform scoring in high-throughput top down proteomics. J Proteome Res. 2014; 13:3231–3240. [PubMed: 24922115]
5. Ntai I, Kim K, Fellers RT, Skinner OS, Smith ADt, Early BP, Savaryn JP, LeDuc RD, Thomas PM, Kelleher NL. Applying label-free quantitation to top down proteomics. Anal Chem. 2014; 86(10): 4961–4968. [PubMed: 24807621]
6. Ahlf DR, Thomas PM, Kelleher NL. Developing top down proteomics to maximize proteome and sequence coverage from cells and tissues. Curr Opin Chem Biol. 2013; 17(5):787–794. [PubMed: 23988518]
7. Savaryn JP, Catherman AD, Thomas PM, Abecassis MM, Kelleher NL. The emergence of top-down proteomics in clinical research. Genome Med. 2013; 5(6):53. [PubMed: 23806018]
8. Meiring HD, van der Heeft E, ten Hove GJ, de Jong APJM. Nanoscale Lc–Ms (N): technical design and applications to peptide and protein analysis. Journal of Separation Science. 2002; 25(9):557–568.
9. Unger KK, Ditz R, Machtejevas E, Skudas R. Liquid chromatography—its development and key role in life science applications. Angew Chem Int Ed. 2010; 49(13):2300–2312.
10. Ye L, Landen WO, Eitenmiller RR. Comparison of the column performance of narrow-bore and standard-bore columns for the chromatographic determination of alpha-, beta-, gamma-, and delta-tocopherol. J Chromatogr Sci. 2001; 39(1):1–6. [PubMed: 11206908]
11. Emmett MR, White FM, Hendrickson CL, Shi SD, Marshall AG. Application of micro-electrospray liquid chromatography techniques to Ft-Icr Ms to enable high-sensitivity biological analysis. J Am Soc Mass Spectrom. 1998; 9(4):333–340. [PubMed: 9879363]
12. Luo Q, Tang K, Yang F, Elias A, Shen Y, Moore RJ, Zhao R, Hixson KK, Rossie SS, Smith RD. More sensitive and quantitative proteomic measurements using very low flow rate porous silica monolithic Lc columns with electrospray ionization-mass spectrometry. J Proteome Res. 2006; 5(5):1091–1097. [PubMed: 16674098]
13. Catherman AD, Li M, Tran JC, Durbin KR, Compton PD, Early BP, Thomas PM, Kelleher NL. Top down proteomics of human membrane proteins from enriched mitochondrial fractions. Anal Chem. 2013; 85(3):1880–1888. [PubMed: 23305238]
14. Morand K, Talbo G, Mann M. Oxidation of peptides during electrospray-ionization. Rapid Commun Mass Spectrom. 1993; 7(8):738–743. [PubMed: 8374164]
15. Shacter E. Quantification and significance of protein oxidation in biological samples. Drug Metab Rev. 2000; 32(3–4):307–326. [PubMed: 11139131]
16. Boys BL, Kuprowski MC, Noel JJ, Konermann L. Protein oxidative modifications during electrospray ionization: solution phase electrochemistry or corona discharge-induced radical attack? Anal Chem. 2009; 81(10):4027–4034. [PubMed: 19374432]
17. Chakravarti B, Chakravarti DN. Oxidative modification of proteins: age-related Changes. Gerontology. 2007; 53(3):128–139. [PubMed: 17164550]
18. Wright A, Hawkins CL, Davies MJ. Singlet oxygen-mediated protein oxidation: evidence for the formation of reactive peroxides. Redox Rep. 2000; 5(2–3):159–161. [PubMed: 10939303]
19. Wright A, Bubb WA, Hawkins CL, Davies MJ. Singlet oxygen-mediated protein oxidation: evidence for the formation of reactive side chain peroxides on tyrosine residues. Photochem Photobiol. 2002; 76(1):35–46. [PubMed: 12126305]

20. Chen YR, Deterding LJ, Sturgeon BE, Tomer KB, Mason RP. Protein oxidation of cytochrome C by reactive halogen species enhances its peroxidase activity. J Biol Chem. 2002; 277(33):29781–29782. [PubMed: 12050149]
21. Smith JD. Apolipoprotein a-I and its mimetics for the treatment of atherosclerosis. Curr Opin Investig Drugs. 2010; 11(9):989–996.
22. Duverger N, Kruth H, Emmanuel F, Caillaud JM, Viglietta C, Castro G, Tailleux A, Fievet C, Fruchart JC, Houdebine LM, Denefle P. Inhibition of atherosclerosis development in cholesterol-fed human apolipoprotein a-I-transgenic rabbits. Circulation. 1996; 94(4):713–717. [PubMed: 8772693]
23. McQueen MJ, Hawken S, Wang X, Ounpuu S, Sniderman A, Probstfield J, Steyn K, Sanderson JE, Hasani M, Volkova E, Kazmi K, Yusuf S. Investigators, I. s., lipids, lipoproteins, and apolipoproteins as risk markers of myocardial infarction in 52Countries (the interheart study): a case-control study. Lancet. 2008; 372(9634):224–233. [PubMed: 18640459]
24. Pankhurst G, Wang XL, Wilcken DE, Baernthaler G, Panzenbock U, Raftery M, Stocker R. Characterization of specifically oxidized apolipoproteins in mildly oxidized high density lipoprotein. J Lipid Res. 2003; 44(2):349–355. [PubMed: 12576517]
25. Bergt C, Pennathur S, Fu X, Byun J, O'Brien K, McDonald TO, Singh P, Anantharamaiah GM, Chait A, Brunzell J, Geary RL, Oram JF, Heinecke JW. The myeloperoxidase product hypochlorous acid oxidizes hdl in the human artery wall and impairs abca1-dependent cholesterol transport. Proc Natl Acad Sci U S A. 2004; 101(35):13032–13037. [PubMed: 15326314]
26. Shao B, Oda MN, Bergt C, Fu X, Green PS, Brot N, Oram JF, Heinecke JW. Myeloperoxidase impairs abca1-dependent cholesterol efflux through methionine oxidation and site-specific tyrosine chlorination of apolipoprotein a-I. J Biol Chem. 2006; 281(14):9001–9004. [PubMed: 16497665]
27. Mateos-Caceres PJ, Garcia-Mendez A, Lopez Farre A, Macaya C, Nunez A, Gomez J, Alonso-Orgaz S, Carrasco C, Burgos ME, de Andres R, Granizo JJ, Farre J, Rico LA. Proteomic analysis of plasma from patients during an acute coronary syndrome. J Am Coll Cardiol. 2004; 44(8):1578–1583. [PubMed: 15489088]
28. Fernandez-Irigoyen J, Santamaria E, Sesma L, Munoz J, Riezu JI, Caballeria J, Lu SC, Prieto J, Mato JM, Avila MA, Corrales FJ. Oxidation of specific methionine and tryptophan residues of apolipoprotein a-I in hepatocarcinogenesis. Proteomics. 2005; 5(18):4964–4972. [PubMed: 16252306]
29. Shao B. Site-specific oxidation of apolipoprotein a-i impairs cholesterol export by abca1, a key cardioprotective function of Hdl. Biochim Biophys Acta. 2012; 1821(3):490–501. [PubMed: 22178192]
30. von Eckardstein A, Funke H, Henke A, Altland K, Benninghoven A, Assmann G. Apolipoprotein a-I variants. Naturally occurring substitutions of proline residues affect plasma concentration of apolipoprotein a-I. J Clin Invest. 1989; 84(6):1722–1730. [PubMed: 2512329]
31. Ladias JA, Kwiterovich PO Jr, Smith HH, Karathanasis SK, Antonarakis SE. Apolipoprotein A1 baltimore (Arg10—Leu), a new apoa1 variant. Hum Genet. 1990; 84(5):439–445. [PubMed: 2108924]
32. Vigushin DM, Gough J, Allan D, Alguacil A, Penner B, Pettigrew NM, Quinonez G, Bernstein K, Booth SE, Booth DR, et al. Familial nephropathic systemic amyloidosis caused by apolipoprotein Ai variant Arg26. Q J Med. 1994; 87(3):149–154. [PubMed: 8208902]
33. Huang W, Sasaki J, Matsunaga A, Nanimatsu H, Moriyama K, Han H, Kugi M, Koga T, Yamaguchi K, Arakawa K. A novel homozygous missense mutation in the Apo a-I gene with Apo a-I deficiency. Arterioscler Thromb Vasc Biol. 1998; 18(3):389–396. [PubMed: 9514407]
34. Vellaichamy A, Tran JC, Catherman AD, Lee JE, Kellie JF, Sweet SM, Zamdborg L, Thomas PM, Ahlf DR, Durbin KR, Valaskovic GA, Kelleher NL. Size-sorting combined with improved nanocapillary liquid chromatography-mass spectrometry for identification of intact proteins up to 80 Kda. Anal Chem. 2010; 82(4):1234–1244. [PubMed: 20073486]

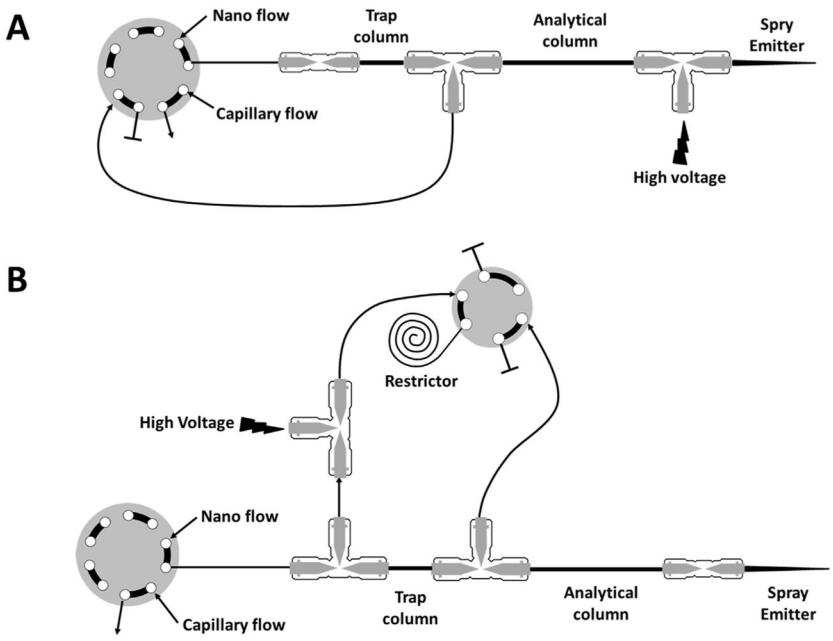

Fig. 1. Conventional LC capillary tubing and LPOx configuration

Conventional capillary plumbing consists of a trap column, vented tee, analytical column, high voltage tee and spray emitter in that order (A). In the LPOx configuration, there is an additional non-conductive switching valve between two vented tees and a restrictor is installed to control the split LC flow at the first vented tee. The location of the high voltage tee (HVT) is between the first vented tee and restrictor (B).

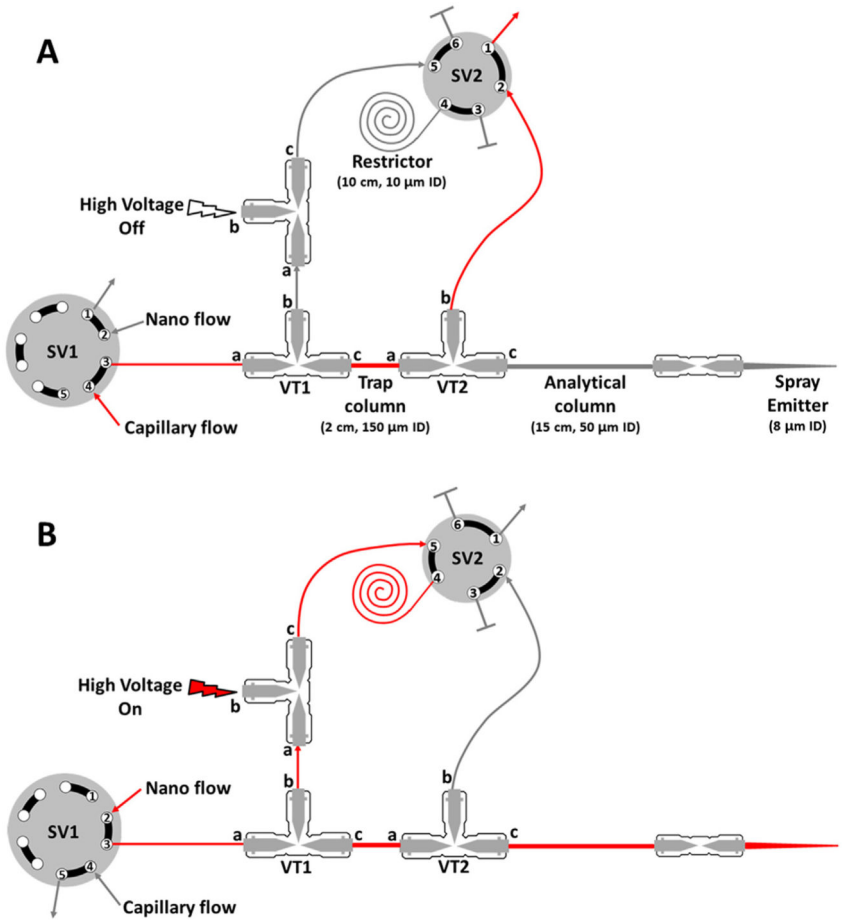

Fig. 2. Diagrams of LPOx plumbing

During the loading phase, sample from the auto sampler can be enriched on trap column via capillary flow through VT1 (a → c) and waste can be removed through VT2 (a → c) linked to SV2 (2 → 1) (A). In this step, high voltage for ESI is off. After the valve position of SV1 is changed, one stream of the split nano flow can go through VT1 (a → b), HVT (a → c), the restrictor on SV2 (5 → 4), and waste out. The other nano flow stream can move through VT1 (a → c), VT2 (a → c), analytical column, and spray emitter in to the MS. In this step, high voltage is applied and electrospray ionization can occur at the end of the spray emitter (B).

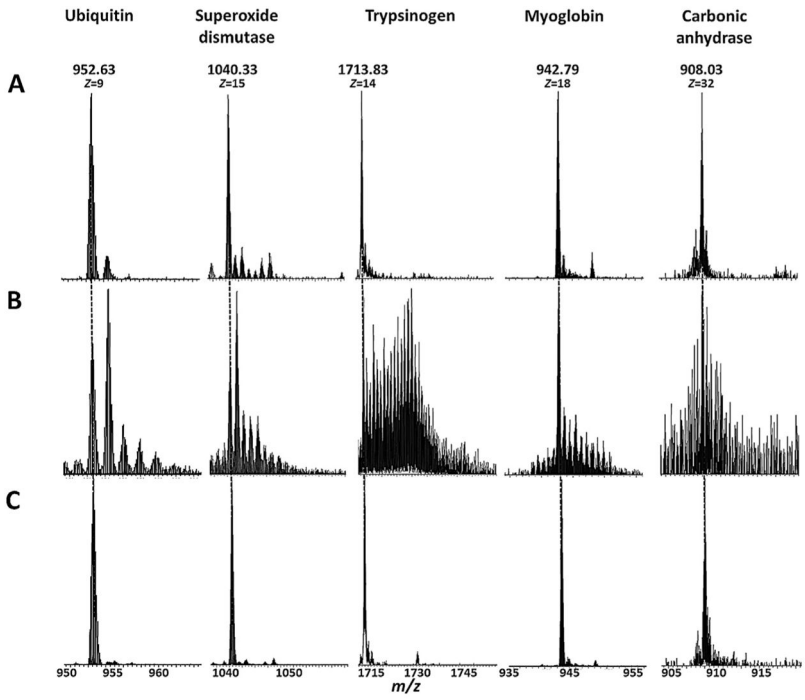

Fig. 3. Zoomed spectra of five intact proteins in three LC capillary settings

FT-MS1 spectra for five standard proteins were acquired in three conditions (75 μm (A) and 50 μm I.D. (B) analytical column in a conventional capillary setting and 50 μm I.D. column in the LPOx configuration (C)) and zoomed peaks of specific charge states of each protein are shown. The Y axis of each plot is relative intensity. Dotted vertical lines in the spectra indicate the un-oxidized protein peaks.

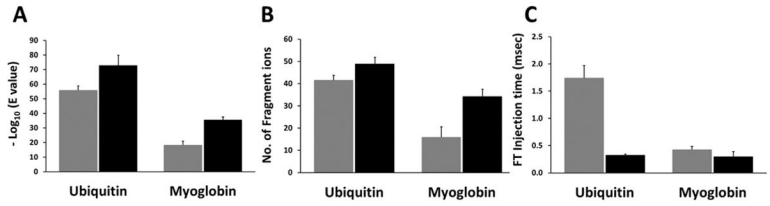

Fig. 4. Comparison of the conventional setting and LPOx configuration in data quality

The number of fragment ions (*b*- and *y*- ions only) reported by ProSightPC analysis, and FT injection time of ubiquitin and myoglobin in two conditions (50 μm I.D. column with the conventional capillary setting (gray bar) and 50 μm I.D. column with the LPOx configuration (black bar) were compared. The standard error of each condition was calculated from triplicate runs and is shown above in the bar graph.

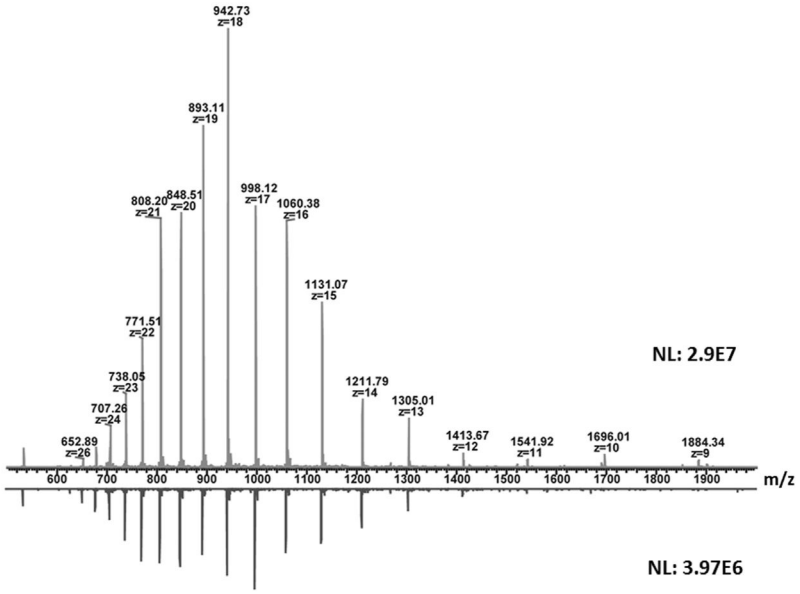

Fig. 5. Comparison of myoglobin peak intensity between the conventional setting with 75 μm I.D. and LPOx with a 50 μm I.D. column

The 5 min-averaged FT-MS1 spectrum for myoglobin from the LPOx configuration with a 50 μm I.D. column (upper spectrum) and from the conventional plumbing with a 75 μm I.D. column (lower spectrum) is shown in a mirrored, reflective manner. The *m*/*z* and the charge states of each peak are shown at the tip of each peak.

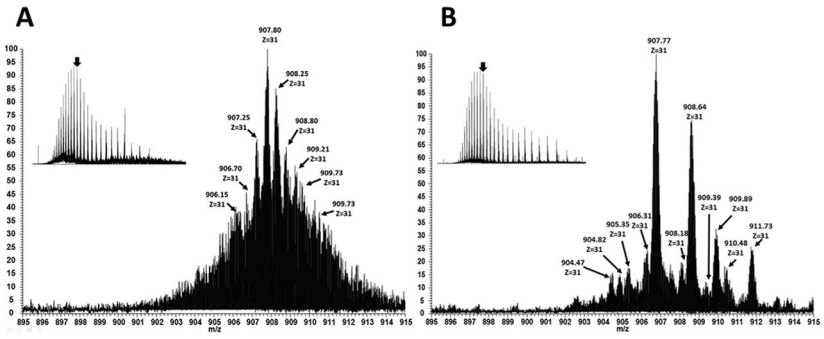

Fig. 6. Comparison of the Apolipoprotein A1 spectrum in the conventional setting with a 75 μm I.D. column and the LPOx configuration with a 50 μm I.D. column

Purified apolipoprotein A1 from human serum was analyzed using both the 75 μm I.D. column with conventional capillary plumbing (A) and 50 μm I.D. column with the LPOx configuration (B). From the 5 min-averaged FT–MS1 spectra (inlet, *m*/*z* range: 500–2000), the MS1 spectra ranging from 895 to 915 *m*/*z* were zoomed in on to view the 31+ charge state proteoform peaks (black arrow in inlet). The *m*/*z* and charge states of each peak are shown above the peak and Y-axis in A and B are the normalized level of intensity.

Table 1

Percentage of oxidation for 5 standard proteins.

% Of oxidation	Conventional configuration		LPOX configuration
Protein	**75 μm I.D.**	**50 μm I.D.**	**50 μm I.D.**
Ubiquitin	12.41	73.36	3.06
Superoxide	40.58	80.75	10.34
Trypsinogen	7.64	93.56	2.08
Myoglobin	16.02	68.84	6.06
Carbonic anhydrase	17.84	76.10	5.37

Peak areas of each protein ions in 3 conditions were measured using Xcalibur software and percentage of oxidation was calculated. Percentage of oxidation was calculated by dividing sum of oxidized protein peak area with sum of total peak area.